DESIGN AND IMPLEMENTATION OF UNDERWATER ACOUSTIC MODEM

A THESIS

Submitted by

SURIYA N	**2019504595**
PRANAV SREENIVAS R	**2019504562**
KOUSHIK M	**2019504540**

On partial fulfillment for the award of the degree of

BACHELOR OF ENGINEERING

IN

DEPARTMENT OF ELECTRONIC ENGINEERING

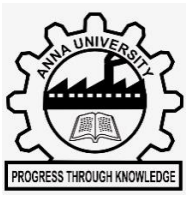

MADRAS INSTITUE OF TECHNOLOGY

ANNA UNIVERSITY: CHENNAI 600 044

May 2023

ANNA UNIVERSITY : CHENNAI 600 044

BONAFIDE CERTIFICATE

Certified that this project **"DESIGN AND IMPLEMENTATION OF UNDERWATER ACOUSTIC MODEM"** is the bonafide work of

SURIYA N	**2019504595**
PRANAV SREENIVAS R	**2019504562**
KOUSHIK M	**2019504540**

who carried out the project work under my supervision. Certified further, that to the best of my knowledge the work reported herein does not form any other thesis of dissertation on the basis of which a degree or award was conferred on an earlier occasion on this or any other candidate.

SIGNATURE

Dr. P. INDUMATHI
HEAD OF THE DEPARTMENT
Professor,
Department of Electronics Engineering,
Madras Institute of Technology,
Anna University,
Chennai - 600 044

SIGNATURE

Dr. G. SUMITHRA
SUPERVISOR
Associate Professor,
Department of Electronics Engineering,
Madras Institute of Technology,
Anna University,
Chennai - 600 044

ABSTRACT

Underwater Communication (UWC) is difficult to implement than standard atmosphere communication, due to the erratic nature of the underwater environment. Acoustic waves are used for Underwater Communication as they have the least attenuation rate than Radio Frequency (RF) Waves and Optical Waves and hence Underwater Acoustic Communication (UWAC) has been the basis for to setting up underwater networks. Present day solutions for setting up Underwater Acoustic Communication, involve transfer of data as Acoustic Signals between Underwater Acoustic Modems (UWAM). The design for a low cost Underwater Acoustic Modem that is portable and cost-effective and reliable has been proposed. The modem also features a low-noise and low-power design, enabling it to operate efficiently and reliably in harsh underwater conditions. The modulation technique used is Frequency Shift Keying (FSK). This design also prioritizes reliability over performance for effective communication. Furthermore, the modem is designed to be robust in order to withstand the harsh environment of the aquatic environment.

TABLE OF CONTENTS

LIST OF TABLES

LIST OF FIGURES

LIST OF SYMBOLS

μ	Signal Spreading pattern medium constant
α	Frequency Dependent Medium constant
π	pi (~3.1415)
e	Euler's number (~2.71828)

LIST OF ABBREVIATION

UAM	Underwater Acoustic Modem
SNR	Signal to noise ratio
SL	Source Level
TL	Transmission Loss
IT	Signal Intensity
NL	Noise Level
DI	Directivity Index
CMRE	Centre for Maritime Research and Experimentation
RF	Radio Frequency
ADC	Analog to Digital Converter
NATO	North Atlantic Treaty of Organization
FGPA	Field Programmable Gate Array
GND	Ground
Tx	Transmitter
Rx	Receiver
FM	Frequency Modulation
FSK	Frequency Shift Keying
FH-FSK	Frequency Hoping Spread Spectrum
In-Amp	Instrumentation Amplifier
Op Amp	Operational Amplifier
PZT	Lead zirconate titanate
PCB	Printed Circuit Board
EDA	Electronic Design Automation
CRC	Cyclic Redundancy Check
UWAC	Underwater Acoustic Communication
OFDM	Orthogonal Frequency Division Multiplexing
UA	Underwater Acoustic
ARM	Advanced RISC Machine

DSSS	Direct Sequence Spread Spectrum
SDR	Software Defined Radio
CPFSK	Continuous Phase Frequency Shift Keying
DFT	Discrete Fourier Transform
DSP	Digital Signal Processor
RTOS	Real Time Operating System
MCU	Microcontroller Unit
PSK	Phase Shift Keying
QPSK	Quadrature Phase Shift Keying
LOS	Line of Sight
NLOS	Non-Line of Sight

ACKNOWLEDGEMENT

We primarily express our gratitude to **Dr.J.Prakash**, Dean, Madras Institute of Technology, Chennai 600044. We wish to express our gratitude to **Dr.P.Indumathi,** Professor and Head, Department of Electronics Engineering, Madras Institute of Technology, Chennai- 600044. We would also like to express our gratitude to **Mrs. K.Karthika** as our Project Coordinator.

We are grateful for **Dr.G.Sumithra**, Associate Professor, for providing this opportunity to undertake this project. Her guidance and motivation, and introducing us to resource people from communication companies, helped us to explore this field and move our project further ahead. Her guidance has been immeasurable and her advices along the way has helped in remolding our thinking process.

We thank our friends who helped in overcoming various software obstacles we faced during the project. We would immensely thank **Mr.K.Veerappan** for aiding us with the printing of our PCB. We would also like to thank **Mrs.J.Velnayaki**, Professional Assistant for helping us in the laboratory to test our circuits.

We would like to express our gratitude to everyone currently working on this technology and also to the future generations, whom we bet on to make the future a better place through this project. Thank you everyone.

PLACE : Chennai **SURIYA N** **2019504595**

DATE : **PRANAV SREENIVAS R** **2019504562**

KOUSHIK M **2019504540**

CHAPTER 1

INTRODUCTION

1.1 The need for an Underwater Acoustic Modem

Presently, there is a growing global need for Underwater Wireless Communication. This technology finds applications in various areas such as autonomous underwater vehicles, where the Underwater Acoustic Modem (UAM) can be integrated into the vehicle, resulting in a portable mobile network with a limited range. This network can be utilized for tasks such as coastal surveillance and monitoring water pollution, among others.

For achieving these applications, establishing a reliable communication between UAM's is mandatory and must also overcome various underwater environment problems for a successful transmission of message underwater.

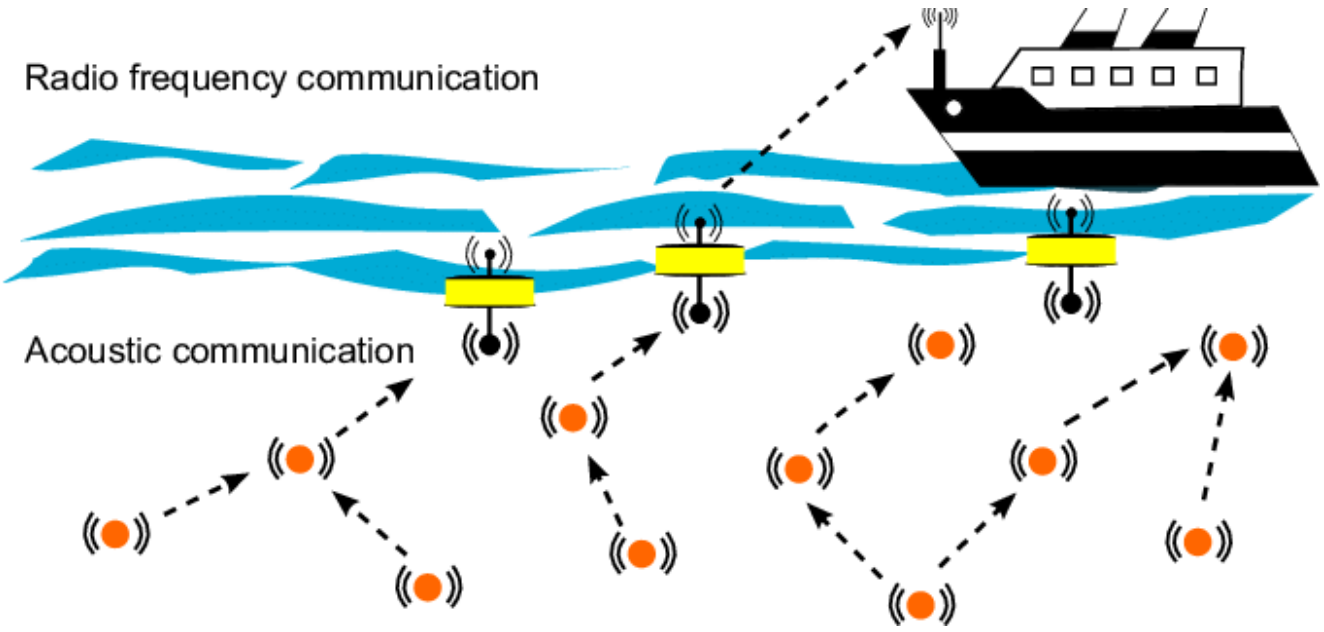

Figure 1.1 Underwater Communication Network [41]

Common wireless communication methods that use atmosphere channel mostly rely on Radio Frequency (RF) signals for communication. They ensure high data rate, large bandwidth but quickly attenuate in the range of 10 meters and thus it cannot be used underwater. We can infer from Table 1.1 that underwater channel offers less data rate comparing to RF and optical communication and higher latency, but it has used widely because of its least attenuation thereby greater range (>1 km). which could be useful in wireless link in shallow water. Thus, the modem is designed to be of low cost and must also ensure the for a reliable transmission of data underwater as it has lower attenuation.

To encourage research in this technology, most of resources planned for this project are not proprietary and are also not difficult to find, thereby enabling the future generations to work on this and upgrade the existing design. Most of the researches are being done in shallow water (about 100m depth) and hence this modem will be designed to work in shallow water conditions.

Table 1.1 Comparison between existing underwater wireless technologies

PARAMETERS	**ACOUSTIC**	**RF**	**OPTICAL**
ATTENUTATION	0.1 dB/m -4 dB/m	3.5 dB/m - 5 dB/m	0.39 dB/m -11dB/m
DATA RATE	in Kbps	in Mbps	in Gbps
BANDWIDTH	1KHz-100 KHz	MHz	10 -150 MHz
FREQUENCY	10-15 KHz	30-300 KHz	10^{12}-10^{15} Hz
PROPAGATION SPEED	1500 m/s	2.255 x 10^{8} m/s	Same as RF
DISTANCE	<20 km	<10 m	<100 m
LATENCY	High	Moderate	Low

1.2 Challenges faced in Underwater Acoustic Communication

Establishing a reliable Underwater Acoustic Communication is difficult due to the channel conditions that are faced during transmission of an Acoustic Signal. These challenges include: -

- Inter-Symbol Interference
- Attenuation
- Multipath Propagation

1.2.1 Inter-Symbol Interference in Underwater Acoustic Communication

One of the major challenges of UWAC is spreading of the signal due to the erratic nature of the channel. This spreading of the signal, cause Underwater Acoustic (UA) symbols to overlap on each other, thus distorting the signal, thereby resulting in data loss. This overlapping of UA symbol is called as Inter-Symbol Interference and is one of the major problems faced while creating a UWAM for underwater communication.

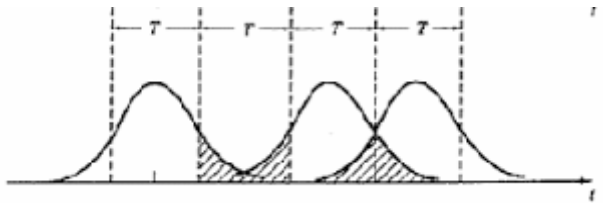

Figure 1.2 Inter Symbol Interference of an Underwater Acoustic Wave [30]

1.2.2 Attenuation in Underwater Acoustic Communication

Attenuation refers to the weakening of the intensity of the acoustic signal as the wave progresses underwater. Acoustic attenuation is a measure of the energy loss of sound propagation in media. This is contributed by 2 major factors: -

- Scattering
- Absorption

The phenomenon by which obstacles or medium fluctuations of small dimensions can modify acoustic wave propagation in the medium. When the waves get reflected by the obstacles, a small amount of energy is absorbed by the obstacle and hence the intensity of the original acoustic signal diminishes.

1.2.3 Multipath Propagation in Underwater Acoustic Communication

Multipath fading occurs due to the acoustic wave taking more than one path from Transmitter to receiver antenna. This reduces intensity of the original signal by splitting its energy among the various multipath waves. This increases attenuation as a greater number of the message wave get attenuated at the same time and resulting wave is distorted and carried very less information.

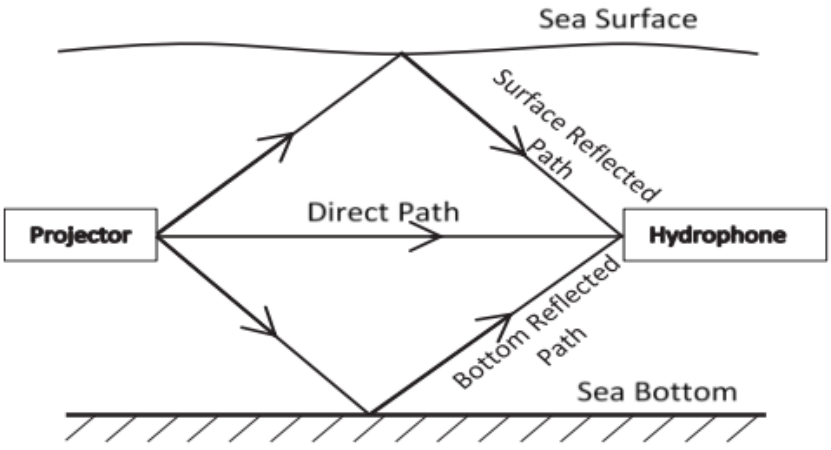

Figure 1.3 Multipath Propagation of an Underwater Acoustic Wave [33]

1.3 Existing Solutions

Most of the existing solutions that exists are expensive and focus on the delivering high-performance industry requirements with limited options for the user in software changes. The current UAM's available in the market are as follows.

The Link Quest Sound Link underwater acoustic modem uses a proprietary broadband acoustic spread spectrum technology to achieve a high data rate with a low bit 13 error rate. The system features advanced hybrid modulation, channel equalization, and environmental adaptation. AquaSent uses OFDM for high performance data transfer, with a proprietary algorithm, and high-speed digital processor.

EvoLogics underwater communication modem based on sweep spread technology, offers a series of different transmission rates and transmission distance modems. The Aquacomm underwater modem has a smaller form factor. Teledyne Benthos also offers a selection of acoustic modems at different transmission rates and distances.

The Micron Data Modem is designed for underwater vehicle control system, small size and lightweight with lower data rate, 40bps, and transmission distance 500m horizontal. High end underwater modems, such as Linkquest, Benthos, and DSPComm modems all cost more than $8000. Lower end modems still cost between $1500 to $3000. Zia Et Al. composed a detailed classifications and analyses of commercial modems.

To summarize, there are a variety of UWAM to choose from but most of them end up being created for large sparse expensive networks and there are still a large number of UWAM's that are under research and not available in the market.
The project-work is outlined as follows. Chapter 2 discusses about the Literature Survey

for the UWAM. Chapter 3 explains the proposed design for the UWAM, followed by the practical considerations for the design of UWAM in Chapter 4. Chapter 5 discusses the simulation outputs and design outputs of the UWAM. Chapter 6 concludes this project-work.

CHAPTER 2
LITERATURE SURVEY

In this chapter, the literature on Underwater Acoustic Modems is presented by highlighting the existing works in modem design, channel modelling and solutions done on them. There are underwater acoustic modems design based on FPGA, ARM, and DSP or combination of those. DSP based modems are used in commercial modem, FPGA modem are used in SDR (Software Defined Radio) which offers flexibility. ARM based modems are low cost, low power modems with limited range.

Benson et.al 2010 [3] designed a low-cost acoustic modem to reduce underwater network cost where small, dense and cheap sensor-nets are needed. Design consists of three parts: underwater transducer whose construction has been discussed, an analog transceiver (power amplifiers and ADC) and digital platform for control and signal processing (using FPGA).

Henrique Manuel Pereira Cabral [4] FPGA based modem uses CPFSK (Continuous Phase Frequency Shift Keying) with DFT (Discrete Fourier Transform) based non-coherent detection method. Operating frequency of modem is around 20-27 KHz achieving data throughput of up to 1500 bps (bits per second).

Software-defined radio is a radio communication system where components that have been traditionally implemented in analog hardware are instead implemented by means of software on a personal computer or embedded system. The key advantage of SDR is its flexibility to change modulation with software. J. G. Duarte-Junior et.al [2] and Emrecan Demirors et.al [1] are based on SDR.

J. G. Duarte-Junior et.al [2] FPGA multi modem design is implemented on EP3C16F484 from Altera with multiple modulation technique (ASK, FSK, PSK) whereas Emrecan Demirors et.al 2014 [1] uses FPGA-Xilinx Spartan 3A-DSP with modulation techniques such as OFDM and DS-SS.

Siyuan Zheng et.al 2019 [6] presented modem for low-cost, compact-sized, underwater platforms like autonomous underwater vehicles (AUVs). Design is based on STM32F4 series processor of Coetex-M4 core with DSSS (Direct Sequence Spread Spectrum) modulation technique.

Benjamin Sherlock et.al 2022 [10] ultra-low cost and ultra-low modem, miniature acoustic modem built around the low-power ARM Cortex M0+ microcontroller. It uses multipath tolerant spread spectrum techniques achieving data rate up to 640 bit/s operating in the frequency range 24-32 KHz.

Won and Park 2012 [13] created an ARM Cortex-M3 embedded omni-directional underwater acoustic micro-modem for underwater communication. A spherical transducer with a resonant frequency of 70 kHz and a diameter of 34 mm is employed for implementation. According to the experiments in the river, it was possible for the modem to send data wirelessly up to 70 m with a data rate of 0.2 kbps while consuming a power of 4.5 watts.

Heungwoo Nam and Sunshin An [11] 2007, created an acoustic modem using ATmega128L MCU for underwater communication, which requires the usage of an acoustic or ultrasonic wave from waterproof ultrasonic sensors instead of a radio wave. Frequency of operation is around 40 KHz and 100 bps is achieved by ASK (Amplitude Shift Keying).

The WHOI Micromodem-2 [19] is a small-footprint, low-power acoustic modem based on the Analog Devices ADSP-BF548BBCZ-5A Blackfin DSP offers data rate from 80-5400 bps, supports various modulation techniques like PSK and FH-FSK. Software

Suresh Kumara and Chanderkant Vatsb [18] thoroughly examine the mechanisms of RF, acoustic, and optical communication, and differentiates them based on parameters such as attenuation, bandwidth, distance, propagation speed, latency, and frequency. Additionally, the workings of an acoustic modem and its components are presented.

Qian Lu et.al 2016 [20] describes various routing protocols for UASNs examines their application-based strategies and proposed schemes for feasibility, rather than the traditional method of using the taxonomy for terrestrial wireless sensor networks.

B.Pranithaa, L.Anjaneyulu Antonio Sánchez, Sara Blanc, Pedro Yuste, Angel Perles and Juan José Serrano [12] outline the physical layer of a new acoustic modem named ITACA. This modem has a unique, energy-saving, asynchronous wake-up system for underwater acoustic transmission. This system is based on a cost-efficient, pre-manufactured RFID peripheral integrated circuit.

Jurdak et.al 2006 [5] took a systematic experimental approach and began with profiling the hardware communication capability in air. This is followed by profiling the same components in water after waterproofing them with elastic membranes. Finally, the experiments evaluate the data transfer capability of the underwater channel by using 8-frequency FSK software modems.

Abolfazl Falahati, Bryan Woodward, and Stephen C. Bateman [16] talk about two models of computer simulation for short-range and long-range propagation. The short-range model indicates that the received signal consists of a direct path and a random path which is caused by boundary scattering. In the long-range model, the signal is composed of multiple time-delayed, randomly propagated components from various paths. Both

models assume that synchronization between transmitter and receiver is ideal, but the channel time delays are realistic. The models show the temporal characteristics of underwater acoustic channels, and are applied for testing the effectiveness of the detection method in simulations.

. Sumithra G and Meganathan D [15] proposed a three-path signal propagation model is to address multipath signal propagation in shallow water applications. This model involves the line of sight (LOS) signal and two non-line of sight (NLOS) signals that contact any point of the channel boundary to reach the receiver. To analyse the effects of the multipath propagation, a simulation is conducted involving a combination of eight possible multipath patterns to estimate the received signal.

Slamet Indriyanto, Anggun Fitrian Isnawati, Jans Hendry, Ian Yosef Matheus Edward [7] have proposed a design for an Underwater Modem using Ultrasonic Sensor JSN SR-04T's Piezoelectric Transducer and XR-2206 and XR2211 for FSK Modulation and Demodulation repectively. The FSK Demodulator XR2211 is replaced by CD4046B in UAM proposed in this paper.

CHAPTER 3

DESIGN OF AN UNDERWATER ACOUSTIC MODEM

3.1 Layout of Underwater Acoustic Modem

The design for the modem has been done keeping flowing of data in mind. Main objective of this project is to send and receive both data (either data sent from the user or the sensor data, which transmit periodically or sporadically) or command to control the state of other underwater modem. From Figure 3.1, it can be seen that modem has two interface i.e from user terminal (Personal computer or server) to the FSK Modem and from Microcontroller and Tx, Rx circuits. Interface from the user terminal to the FSK Modem is established using SPI ports. And similarly interface between microcontroller and Tx Rx circuits are established using UART Tx and Rx pins.

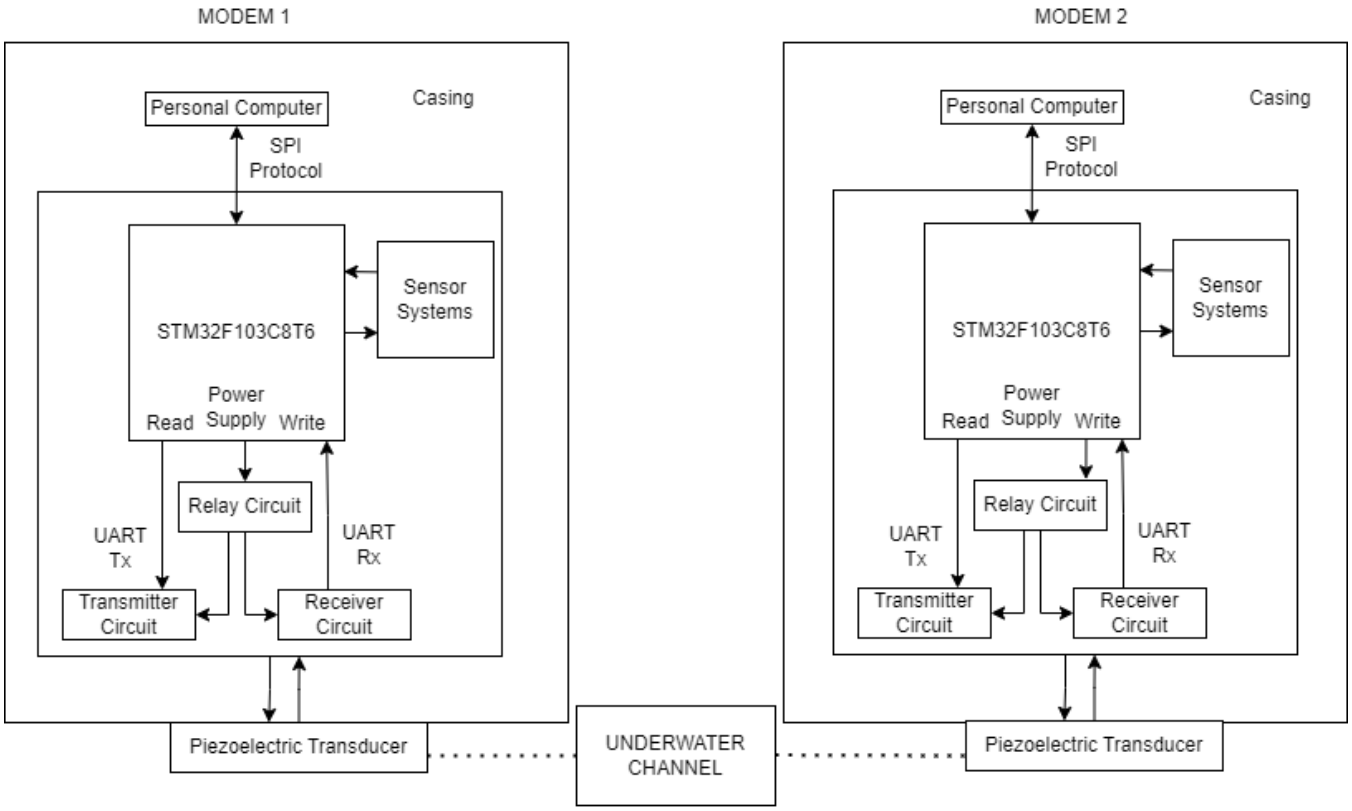

Figure 3.1: Process Flow of UWAM

The design of the UAM consists of a Microcontroller, a Transmitter Circuit, Receiver Circuit, Power Supply Circuit and Piezoelectric Transducer. A Power Shift circuit is used to maintain a stable power. The Power Shift signal function sent to the 5 V Relay is either turned on or off depending on Transmitter or Receiver Circuit. The Default mode of the power shift circuit (Active low) is powering the Receiver (Rx) circuit for constant monitoring of the signal from the Piezoelectric transducer. To transmit the message (either sensor data or custom data from user), the power supply signal is turned to Active High to active the Transmitter circuit, and then data is sent to the microcontroller using the required protocol (SPI/UART/I2C), and the data is sent with the help of UART protocol (where the binary signal is converted to analog signal) to the Transmitter Circuit, which consists of FSK Modulator circuit to convert binary signal to FSK (Frequency shift keying) signal. The FSK signal is sent to Ultrasonic sensor Piezoelectric Transducer which then converts incoming electric signal to acoustic wave, which then propagates through underwater. To receive the message, the UAM checks the state of the Piezoelectric transducer and based on energy threshold, the FSK signal is first passed through an Instrumentation Amplifier circuit, followed by a Bandpass filter circuit and finally the Demodulation circuit to get the required signal from the transmitting side.

3.1.1 Overview of the modules of Underwater Acoustic Modem

The UAM consists of a Transmitter, Receiver, Battery, Battery protection circuit, Piezoelectric transducer, and an MCU unit, all enclosed in a housing as shown in Fig 3.2. The MCU used here is the STM32F103C8T6. Three 3.7V, 2000mAh batteries are used, along with a battery protection circuit. The Piezoelectric transducer acts both as an underwater speaker and a hydrophone.

The Transmitter circuit amplifies the output signal from the controller circuit to the piezoelectric transducer.

The Receiver circuit identifies the received signal from the piezoelectric transducer, amplifies it, filters it, and then decodes it using the controller circuit. The controller circuit adjusts the amplification factor based on the environment, power consumption, and noise levels.

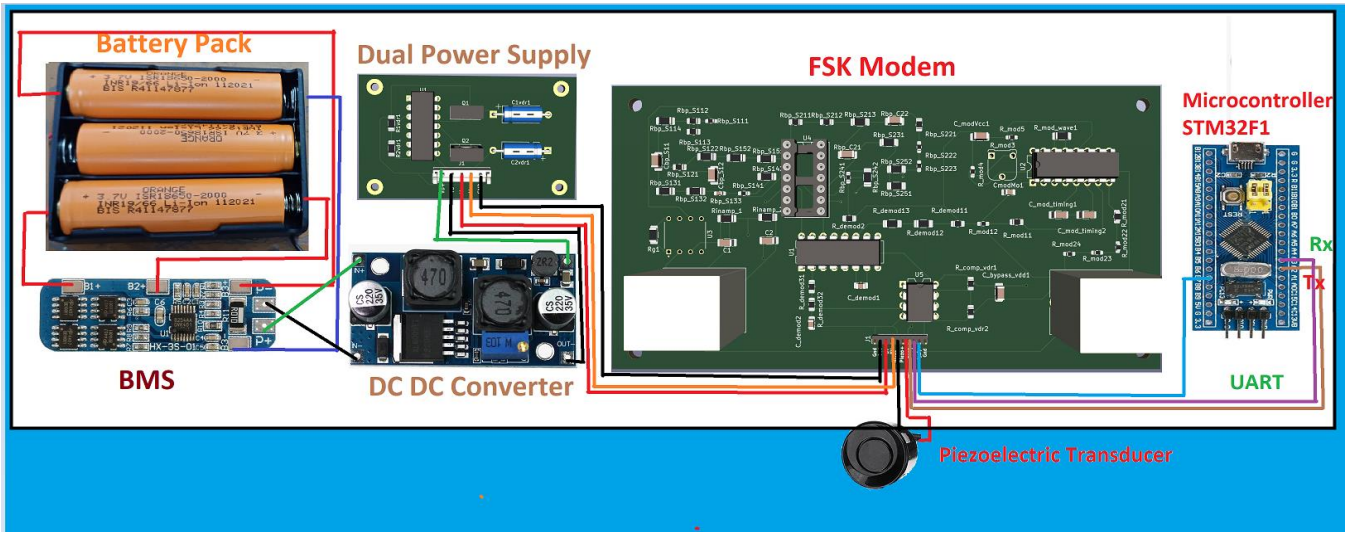

Figure 3.2: - Block Diagram of Underwater Acoustic Modem

3.2 Software involved in the development of the UAM

3.2.1 STMicroelectronics CubeIDE

STMicroelectronics CubeIDE (Integrated Development Environment) is a powerful and intuitive tool used for developing software applications for STM32 microcontrollers. It is an integrated platform that combines the features of STMicroelectronics' STM32CubeMX graphical configurator and Eclipse-based IDE. CubeIDE provides an easy-to-use interface for developing, debugging, and deploying embedded applications much faster.

3.2.2 LT Spice

LT Spice - SPICE-based analog electronic circuit simulator computer software, produced by semiconductor manufacturer Analog Devices. In this project Schematics are test using LT Spice software.

3.2.3 KiCad

KiCad is Open-source EDA (Electronic Design Automation) for Schematic Capture and PCB designing. Here it is used to design PCB. KiCad has default libraries for components/ symbols.

3.3 KiCad schematic of UAM

The circuit was designed using KiCad software. The main components of the PCB are: -

- ▶ Transmitter Circuit
  - FSK Modulator circuit
- ▶ Receiver Circuit
  - In-Amp circuit
  - Bandpass filter circuit
  - FSK Demodulation circuit
- ▶ Dual Rail Power Supply Circuit

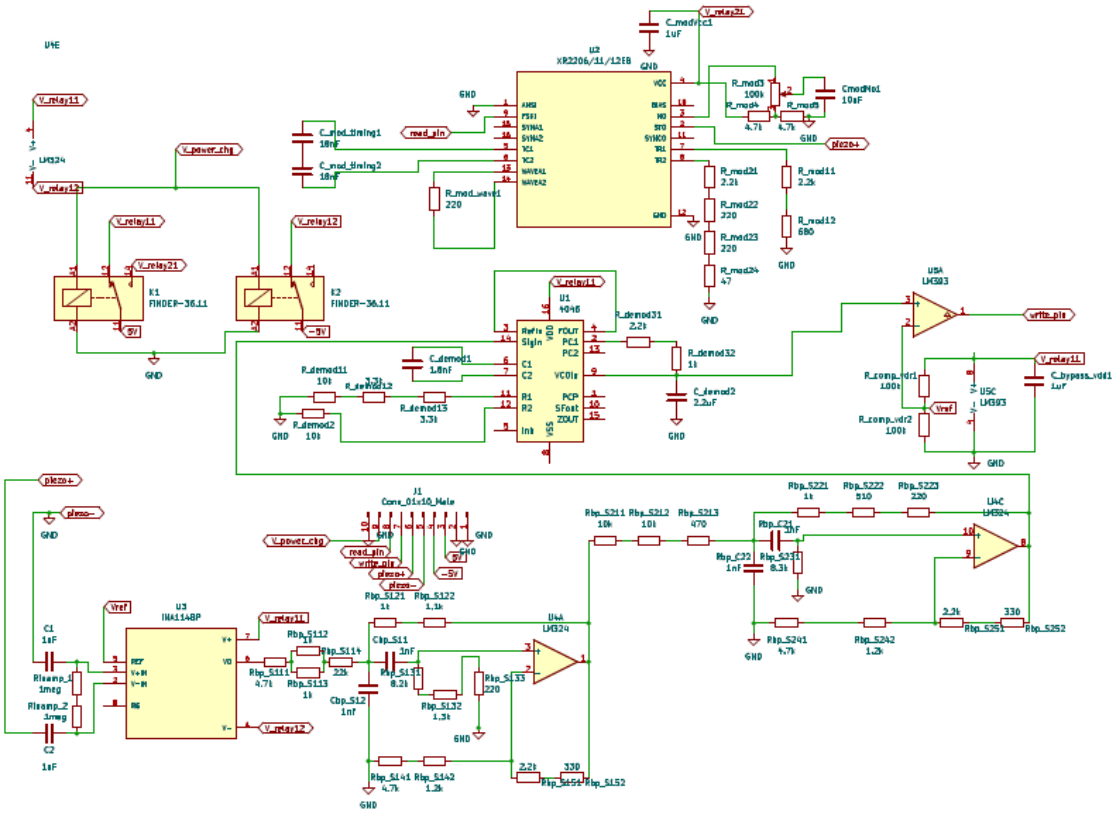

Figure 3.3: - KiCad schematic of the UAM

3.4 Microcontroller used in UAM - STM32F103C8T6

The UAM uses the Microcontroller STM32f103c8t6 for communication with sensors and to function as the central processor of the UAM. The primary benefits conferred by this board reside in its compact dimensions and relatively lower cost.

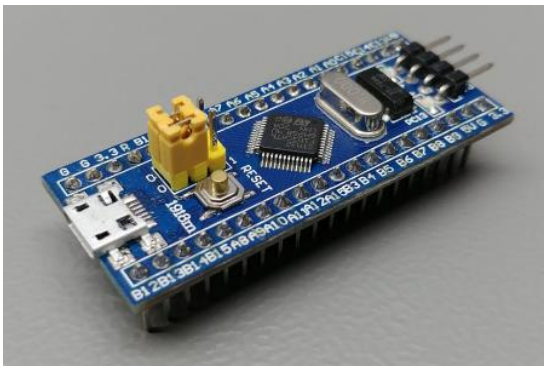

Figure 3.4: - Image of STM32F103C8T6[8]

Table 3.1 highlights few of the specifications of this microcontroller. It has UART, I2C pins data transmission. The SPI and CAN communication protocols are used in this modem to create communication both internal communication in FSK modem and externally from FSK modem to User or Transmitting Receiving (Tx-Rx) circuit.

Table 3.1: - Specifications of STM32F103C8T6

Operating voltage	3.3V
Analog inputs	10
Digital I/O pins	37
DC source/sink from I/O pins	6 mA
Flash memory (KB)	64/128
Frequency (clock speed)	72 MHz (Maximum)
Communication Protocols	I^2C, SPI, UART, CAN, USB

3.5 Modulation Circuit of UAM

The XR-2206 is an integrated circuit that serves as a monolithic function generator. It has the ability to produce various waveforms including high-quality sine, square, triangle, ramp, and pulse waves with great accuracy and stability. An external voltage can be used to modulate the amplitude and frequency of the output waveforms. The frequency of operation can be chosen from an external source within a range of 0.01Hz to more than 1MHz. The circuit in Fig 3.5 is particularly useful for applications such as communication, instrumentation, and function generation where sinusoidal tone, AM, FM, or FSK generation is required. Additionally, the oscillator frequency can be linearly swept across a 2000:1 frequency range with the help of an external control voltage, while maintaining low distortion. The typical drift specification of the circuit is 20ppm/°C.

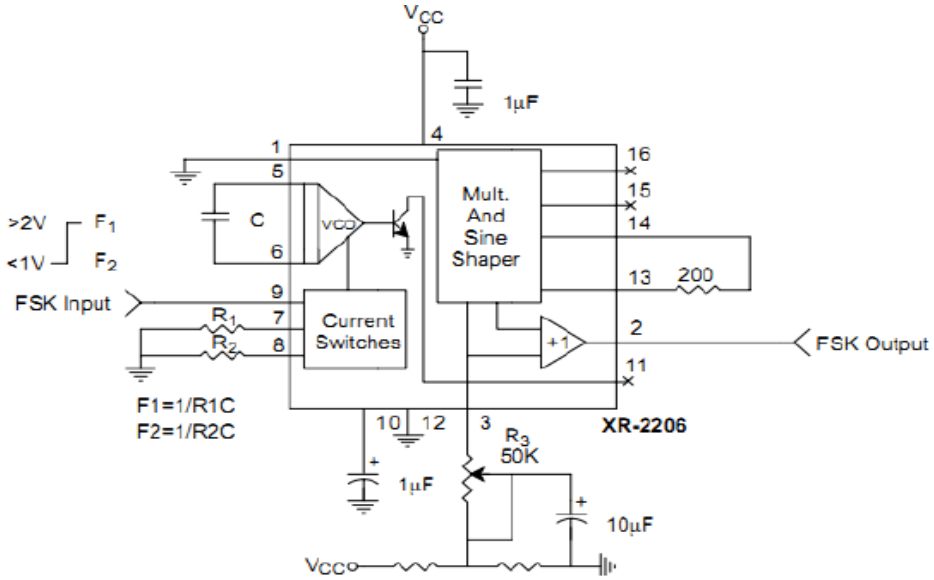

Figure 3.5: - Circuit Diagram of FSK Generation using XR-2206

Figure 3.6: - Image of FSK Generator using XR-2206 [50]

3.6 Demodulation Circuit of UAM

The CD4046 is an integrated circuit that implements a phase-locked loop (PLL) and can function as an FSK (Frequency-Shift Keying) demodulator. As an FSK demodulator, it can detect and demodulate FSK signals that have a broad range of frequency deviation and modulation rates. To achieve this, the FSK input signal is connected to the "VC" pin, which is linked to the voltage-controlled oscillator (VCO) input, shown in Fig 3.7. The demodulated output signal is a DC voltage that is proportionate to the input signal frequency, and it can be processed further or measured with a multimeter. The CD4046 has an operating voltage range of 3V to 15V, making it suitable for different applications. Additionally, it is a low-power device with a power consumption of only a few milliwatts. The CD4046 comes in various package types, including DIP, SOIC, and TSSOP. Apart from its role as an FSK demodulator, the CD4046 can also function as a frequency multiplier/divider, frequency synthesizer, or other applications that need frequency control or phase-locking.

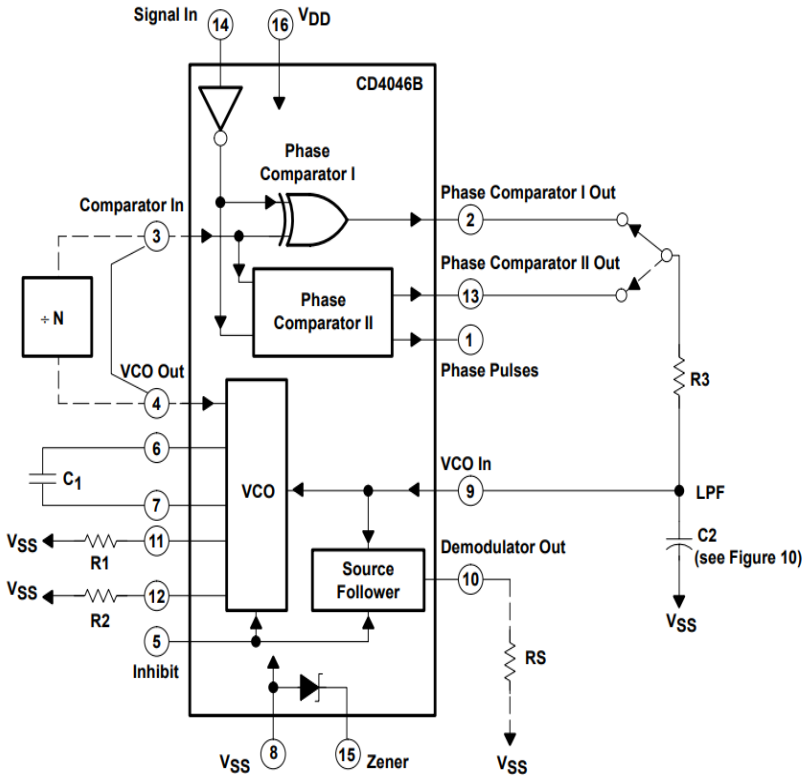

Figure 3.7: - Circuit Diagram for FSK Demodulation using CD4046[51]

Figure 3.8: - Image of FSK Demodulator CD4046B

3.7 Bandpass Filter Circuit of UAM

The LTSpice circuit of Bandpass Filter is shown in Fig 3.9. After the weak input signal is amplified by the instrumentation amplifier, it is important to remove the noise and interference from outside the frequency of interest and is necessary to avoid the noises like Ambient Noise, Thermal Noise and Biological Noise. Filters can be constructed in different topologies. The most popular topology are Multiple Feedback and Sallen Key filter. Multiple Feedback (MFB) filters offer flexibility in filter response and wide bandwidth, but they can be sensitive to component variations and have limited stop-band attenuation. On the other hand, Sallen Key filters are simple to design, have a good frequency response and low component count, but they may have a narrower bandwidth and can be sensitive to component variations. Both filter topologies have their advantages and disadvantages, which are needed to be considered based on specific application requirements. The UAM uses 4th order Butterworth filter. Butterworth gives flat response in passband.

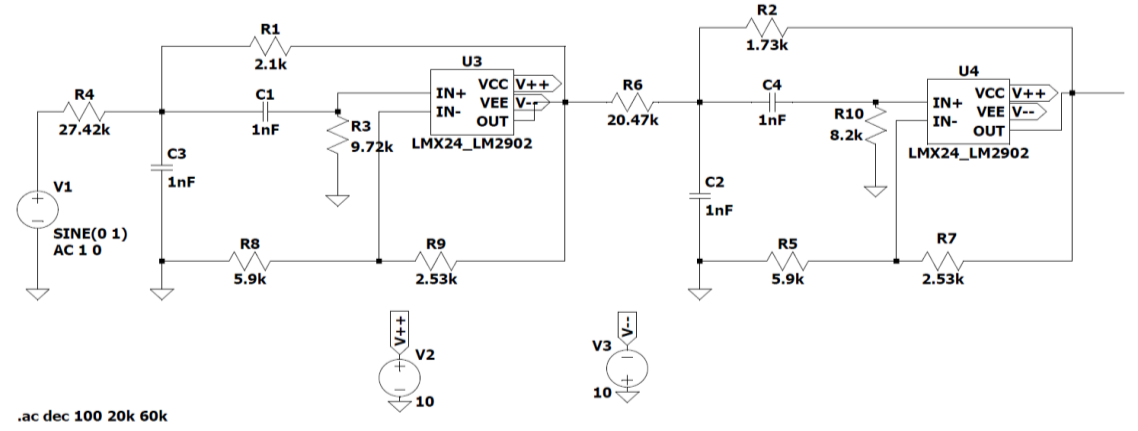

Figure 3.9: - Bandpass Filter Circuit of the UAM

3.8 Dual Rail Power Supply of UAM

This is the LTSpice circuit of Dual Rail Power Supply.

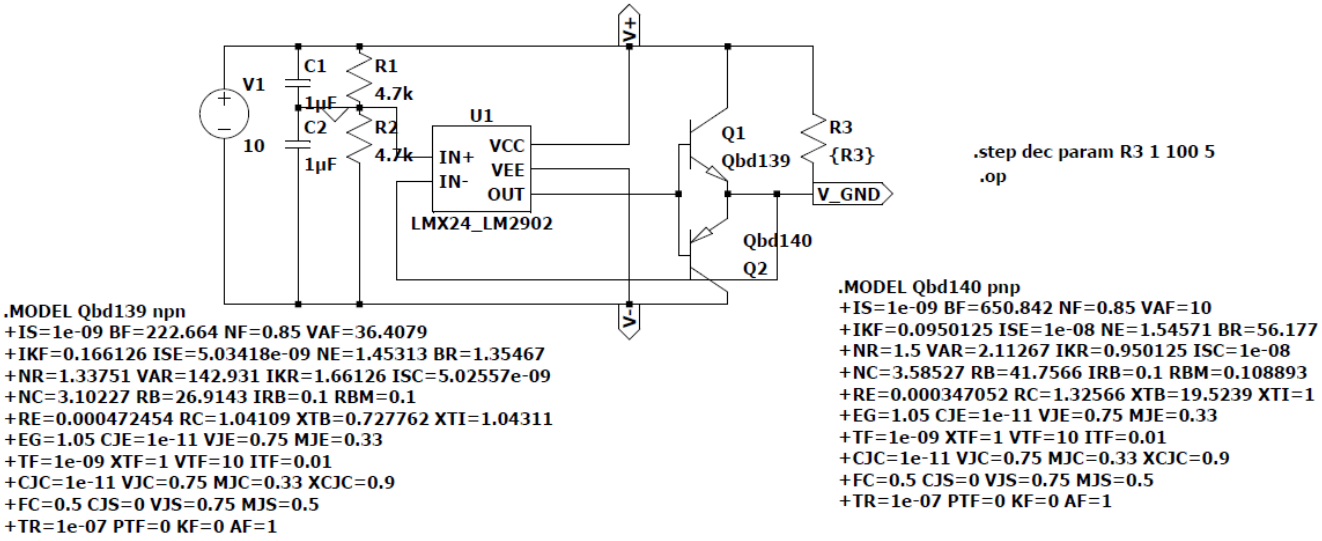

Figure 3.10: - Circuit for Dual Rail Power Supply Circuit of UAM

3.9 Ultrasonic Transducer used in UAM

The JSN-SR0T4 is a waterproof ultrasonic distance/range measurement sensor module with a non-contact range/distance of 25 cm to 450 cm and is very similar to the ultrasonic sensor found in a car bumper. It Operates from a nominal supply voltage of 4.5 V to 5.5 V DC. it typically works with 5.0V DC voltage and requires a maximum of 30 mA current. The Features and Specification of JSN SR-04T: -

- ▶ Operating voltage: DC 5V
- ▶ Quiescent current: 5mA
- ▶ Maximum current draw: 30mA
- ▶ Frequency: 40khz
- ▶ Range: 25cm to 450cm

- Beam Angle: less than 50 degrees
- Working temperature: -10 ~ 70 Celsius
- Storage temperature: -20 ~ 80 Celsius

Figure 3.11: - Ultrasonic Transducer used in UAM [7]

The UAM uses the piezoelectric Transducer of Ultrasonic Transducer, JSN- SR0T4 due to it being inexpensive and readymade.

3.10 Power Supply for UAM

The UAM is powered by three cells in 3S method. The specifications of the cell is as follows: -

- **Capacity:** 2000 mAh
- **Output Voltage:** 3.7V*3 = 11.1 V
- **Maximum Current Capacity:** 4 A
- **Maximum Discharge Current:** 5 C
- **Charging temperature:** 0 – 45°C
- **Discharging Temperature:** 20° – 60°C

Calculating the Maximum Power and Battery Capacity from the specifications, we get,

- **Maximum Power Battery can dissipate** = 3*3.7 V*3*2 A = 66.6 W
- **Battery capacity** = 3 cells * 3.7 V * 2000 mAh = 22.2 Wh

Therefore, Estimated stand-by time = 11.1 hours.

3.11 UART Specification of UAM Communication

```
huart.Instance = USART2;                    //huart is the UART Instance
huart.Init.BaudRate = 2000;
huart.Init.WordLength = UART_WORDLENGTH_8B; //Length is 8 Bits
huart.Init.StopBits = UART_STOPBITS_1;                    //EndofFrame
huart.Init.Parity = UART_PARITY_NONE;
huart.Init.Mode = UART_MODE_RX;
huart.Init.HwFlowCtl = UART_HWCONTROL_NONE;
huart.Init.OverSampling = UART_OVERSAMPLING_16;
```

3.12 Packet Structure of Data sent via the Modem

```
typedef struct packet
{
uint8_t preamble;          //0xA5
uint16_t sync_word;        //0x55AA
uint8_t type;              //0x01
uint8_t length;            //1 Byte
char data[256];            // Character array to store the string data
uint16_t crc;
} packet_t;
```

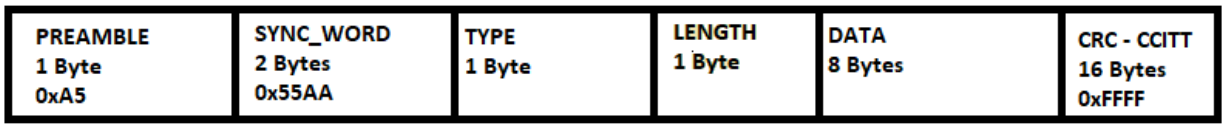

Figure 3.12 Packet Structure of Data

CHAPTER 4
DESIGN OF UNDERWATER ACOUSTIC MODEM

The design parameters for the modulation and demodulation circuits were decided by referring to the respective datasheets of the IC's. The performance of the transducer was tested and the SNR was calculated for the experiment and the calculations relating to that are mentioned in this chapter.

4.1 Technical Specifications for XR2206

FSK Modulation is performed using XR2206 function generator IC. It is used in the modulation circuit to generate FSK signal. The aim of this FSK modulation circuit is to set frequencies of FSK to be 38KHz (f1) for the symbol '0' and 42 KHz for the symbol '1'. The design of the modulation circuit to work under such constraints is done by setting the value for Timing Capacitance (C) and timing Resistances (R_1 and R_2). From the datasheet [52], it can be inferred that the value of Timing Capacitance should be in range of 1000 pf -o 100 µf and the value of timings resistances should be in the range of 1 kilo ohm to 2 mega ohm. Frequency of fsk signals for the symbol 0 (f_1) and symbol 1 (f_2) is given in equation 4.1.

$f_1 = 1/ (R_1 * C)$ (4.1)

$f_2 = 1/(R_2*C)$ (4.2)

Taking C = 9nF and frequency of fsk signals as f_1 = 38 KHz and f_2 = 42 KHz, timings resistance is calculated from the modified form of equation 4.1 and 4.2 as: -

$R_1 = 1/(f_1*C)$ (4.3)

$R_2 = 1/(f_2*C)$ (4.4)

Which gives the value of timing resistance as

$R_1 = 1/(f_1*C) = 1/ (38*10\text{^}3*9*10\text{^}-9) = 2.924$ kilo ohm (4.5)

$R_2 = 1/(f_2*C) = 1/ (42*10\text{^}3*9*10\text{^}-9) = 2.646$ kilo ohm (4.6)

R1 and R2 can be approximated to 2.880 kilo ohm and 2.670 kilo ohm which on equating with equation 4.1 and 4.2 gives 38.58 KHz and 41.61 KHz.

4.2 Technical Specification of IC CD4046

Demodulation is performed using IC CD4046BE. The CD4046BE Phase Lock Loop IC offers two phase comparators i.e., phase comparator 1 and 2. But Phase comparator 1 is built using exclusive or (EX-OR) and digital phase. Phase comparator 1 is preferred in high-speed application despite its inability to differentiate phase between two signals. From Figure 4.1 Voltage Controlled (VCO) can operated either of 2 modes i.e., with offset and without offset. With offset is chosen in this modem design to adjust the lock range (Frequency range where PLL can accurately synchronize input signal.). Required Parameters with value is shown from equation 4.7 to equation 4.12

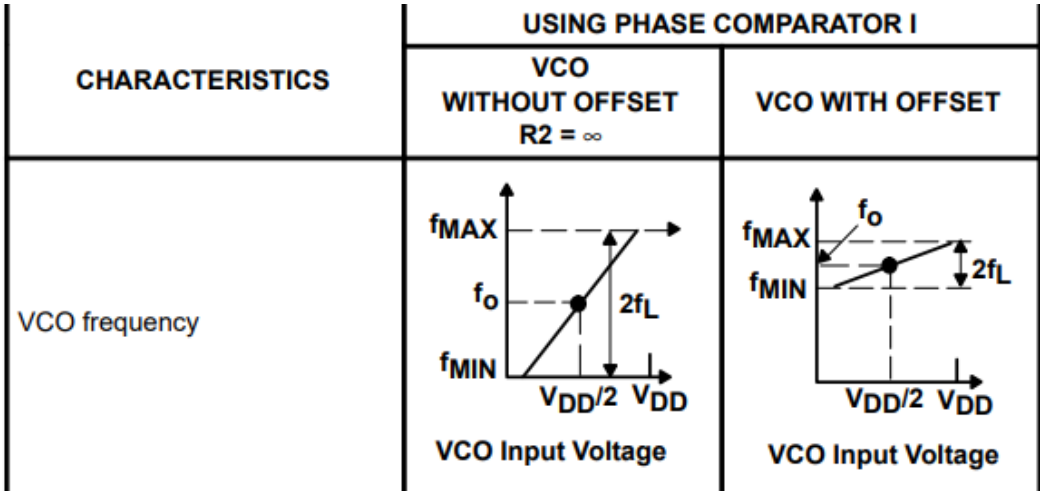

Figure 4.1: - Graph to choose Vco Frequency for Phase comparator [51]

- Center frequency (f_o) = 40 KHz (4.7)
- Minimum frequency for PLL to lock (f_{min}) = 32 KHz (4.8)
- Minimum frequency for PLL to lock (f_{max}) = 48 KHz (4.9)
- Lock Range (f_L) = (48-32)/2 = 8 KHz (4.10)
- Capture Range (f_c) < 7 KHz (4.11)
- Power Supply (V_{DD}) = 5V (4.12)

Figure 4.2 shows the basic circuit for FM Demodulation. And the value of parameters from the figure 4.2 need to calculated are R_1, C_1 for the V_{CO} and R_3, C_2 for the low Pass Filter. Following steps need to done to calculate values of unknown variables.

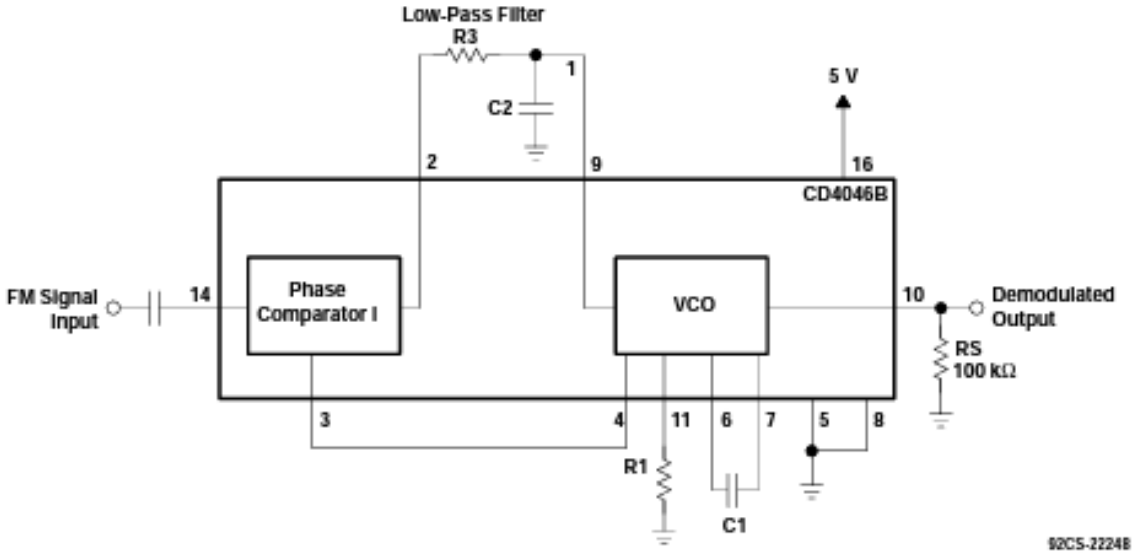

Figure 4.2: - Diagram of CD4046 Demodulator [51]

1. Find C1 for the given value of V_{DD} (5V), R1 (10 k ohm) and fo (40KHz).
2. Find the ratio of R2/R1 for the given f_{max}/f_{min} = 48/32 = 1.5.
3. Find Low Pass Filter parameter values.

Step 1: Graph to calculate C1 in Demodulation Circuit

Let V_{DD} = 5V and R_1 = 10 kilo ohm. Line which satisfies the following criteria is line 3. By setting center frequency (f) as 40 KHz from the graph, C found to be 0.9 nF.

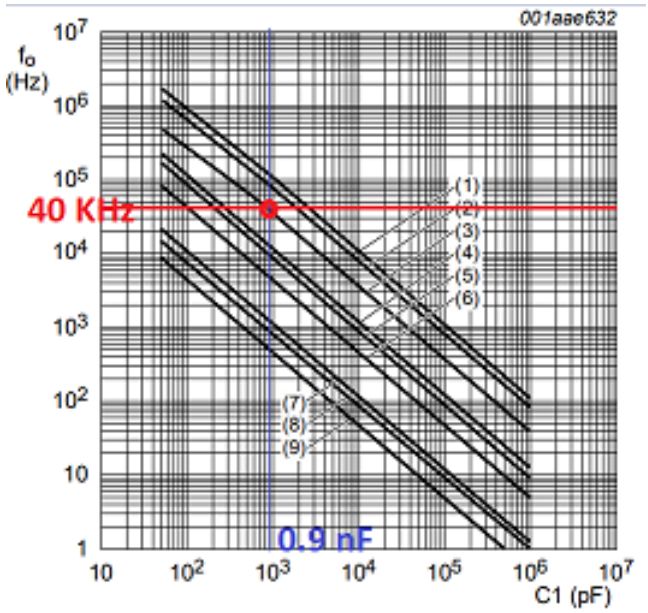

T_{amb} = 25 °C; VCO_IN at 0.5V_{DD}; INH_IN at V_{SS}; R2 = ∞.

Lines (1), (4), and (7): V_{DD} = 15 V;
Lines (2), (5), and (8): V_{DD} = 10 V;
Lines (3), (6), and (9): V_{DD} = 5 V;
Lines (1), (2), and (3): R1 = 10 kΩ;
Lines (4), (5), and (6): R1 = 100 kΩ;
Lines (7), (8), and (9): R1 = 1 MΩ.

Figure 4.3: - Graph depicting C_1 vs f_o [53]

Step 2: - Graph to calculate R1/R2 using VDD = 5V

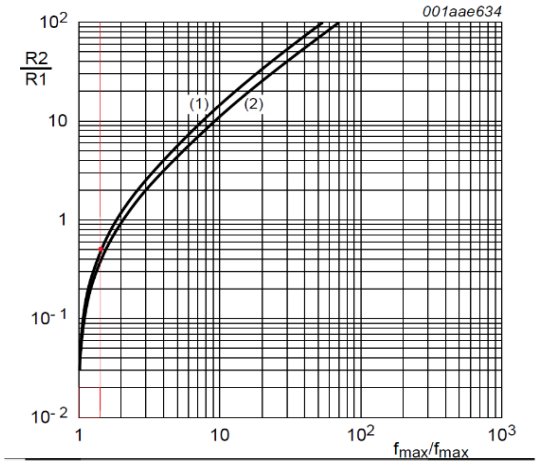

Figure 4.4: - Graph depicting f_{max}/f_{min} Vs R_2/R_1 [53]

We know,

f_{min} = 32 KHz, f_{max} = 48 KHz,

So,

f_{max}/f_{min} = 48KHz/32 KHz = 1.5,

and from fig 4.4, when V_{DD} = 5V,

R1/R2 = 0.6,

Given R1 = 10 K ohm and R2/R1 = 0.6

R2 = R1*0.6 = 6 K ohm

Step 3: - Calculate Low pass filter parameters

The value of capture range of PLL from [53] is given as

$$f_c = \frac{1}{2*\tau_1}\sqrt{\frac{2*\pi*f_L}{\tau_1}} \quad (4.13)$$

Where $\tau_1 = R_3 * C_2$ (4.14)

From trial and error, R_3 and C_2 values are found to be 3.2 kΩ and 2.2 μF to get f_c less than 7KHz.

Substituting , R_3 and C_2 values are found to be 3.2 kΩ and 2.2 μF in equation 4.14 gives

$$f_c = \frac{1}{2*3.2*10^3*2.2*10^{-6}}\sqrt{\frac{2*\pi*8*10^3}{3.2*10^3*2.2*10^{-6}}} = 6001\ Hz \qquad (4.15)$$

4.3 Technical specifications for FSK modulation

The UAM uses Frequency Shift Keying modulation technique for modulation the incoming Binary Signal. It is used due to its reliability in harsh medium conditions.

The Non-Coherent Binary Frequency Shift Keying parameters are [4]: -

- Mark Frequency – 42 KHz
- Space Frequency –38 KHz
- Data Rate – 600 to 2000 bits/second
- Range – around 100 metres

4.4 SNR calculation for simulation

Using Passive Sonar Equation to calculate the final SNR value for a range of 0.24m for the testing of the transducer: -

$$SNR = SL-TL-NL+DI \quad (4.16)$$

In Equation 4.16, SL is the Source Level, TL is the underwater transmission loss, NL is the noise level, and DI is the Directivity Index. The quantities are usually expressed in dB re μPa, where 1 μPa is equivalent to 0.67 x 10-22 Watts/ cm^2. The Reference Power Density Level of 10^{-12} Watts/ m^2 is used, which is the threshold of human hearing to compare our results to the general output of our hardware. The term dB signifies dB re 10^{-12} unless otherwise specified. Due to the use of omnidirectional sensor, the directivity index DI is zero. As highlighted in [5], directing the acoustic energy released from the speakers can improve signal quality significantly

$$\text{Source Level (SL) at 0.24m depth} = 10*\log (I_t/10^{-12}) \quad (4.17)$$

In equation 4.17,

'I_t' is the Intensity of the Signal at 100m depth

$$\text{Signal Intensity } (I_t) \text{ at 0.24m depth} = P_t/ (2* \pi * d*H) \text{ Watts/m}^2 \quad (4.18)$$

In equation 4.18, P_t is Transmitted signal Power (P_t=999.96 dB), H is the depth (H=0.24m).

So, substituting value of P_t and H in equation 4.18,

$I_t = 0.238$ Watts/m^2

Substituting value of I_t is equation 4.17, we get,

Source Level (SL) at 100m depth = 10log (It/10^{-12}) = 10log (3.183) = 113.76 dB

$$\text{Transmission Loss (TL)} = (10 * \mu \log(d)) + (\alpha*d * 10^{-3}) \quad (4.19)$$

In equation 4.19,

'd' is the distance between source and receiver in meters (d=999.96m),

'μ' depends on the signal spreading pattern and in shallow water cases, the value of μ lies somewhere between 1 and 2 (Let μ=1.5).

'α' is the frequency dependent medium absorption coefficient in dB/km and for frequency range between 35 KHz and 50 KHz, $\alpha = 0.504*f - 11.2$ dB/Km.

So, substituting value of d, μ, α in Equation 4.19, we get

$TL = 10*1.5*\log(999.96) + 9.78*221.785*10^{-3}*1000*10^{-3} = 0.85$ dB.

Therefore,

Substituting values of SL, NL, TL and DI in equation 4.19: -

Noise Level (NL)= 30 dB

$SNR = SL - TL - NL = 113.76 - 0.85 - 20 = 92.92$ dB re 10^{-12}

CHAPTER 5

SIMULATION RESULTS

The software simulations of the circuits were performed using LTSpice and the PCB were designed using KiCad software. An experiment was conducted to test the Transducer performance, by connecting one transducer to a Function Generator and another transducer to an Oscilloscope and testing the range and frequency response of the transducer. The results are depicted graphically in Fig 5.1 and 5.2.

5.1 Relationship between Distance the Transducers and Amplitude of the Received Signal

The range of the Transducer was tested for an input voltage of 26.2 V and a Frequency of 40.3 KHz and a Distance vs Amplitude Graph is plotted in Fig 5.1.

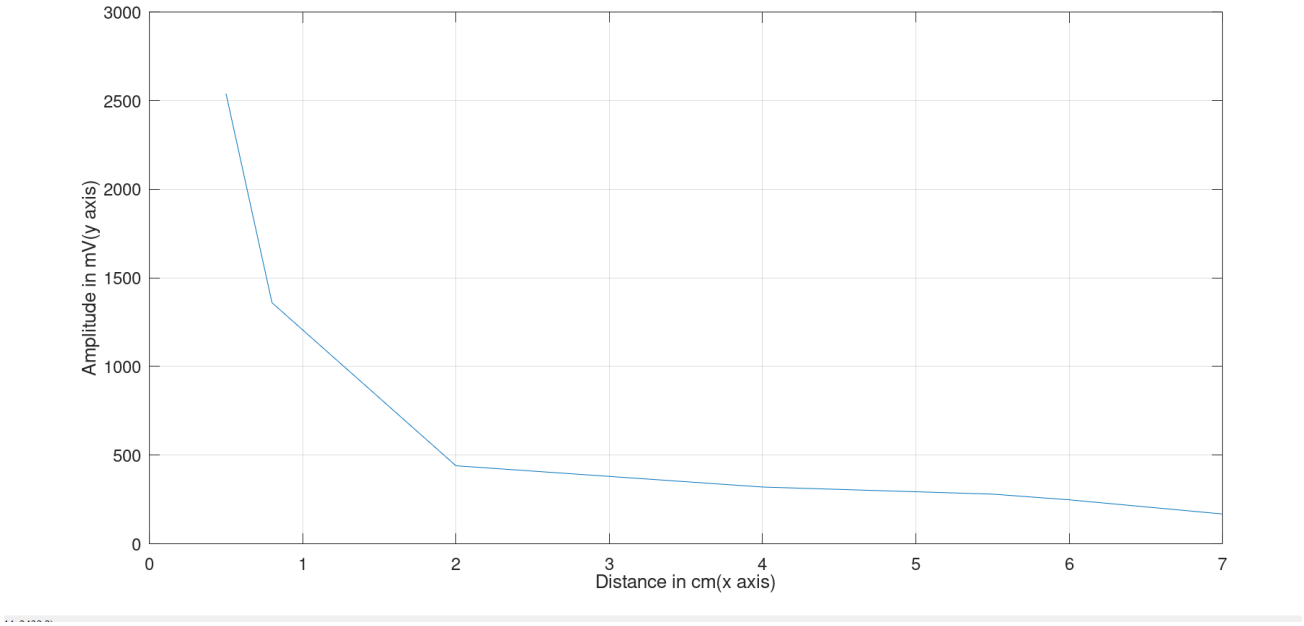

Figure 5.1: - Distance vs Amplitude Graph depicting the Negative and Non-Linear relationship between them.

5.2 Relationship between Distance the Transducers and Amplitude of the Received Signal

The Frequency Response of the Transducer is plotted in Fig 5.2.

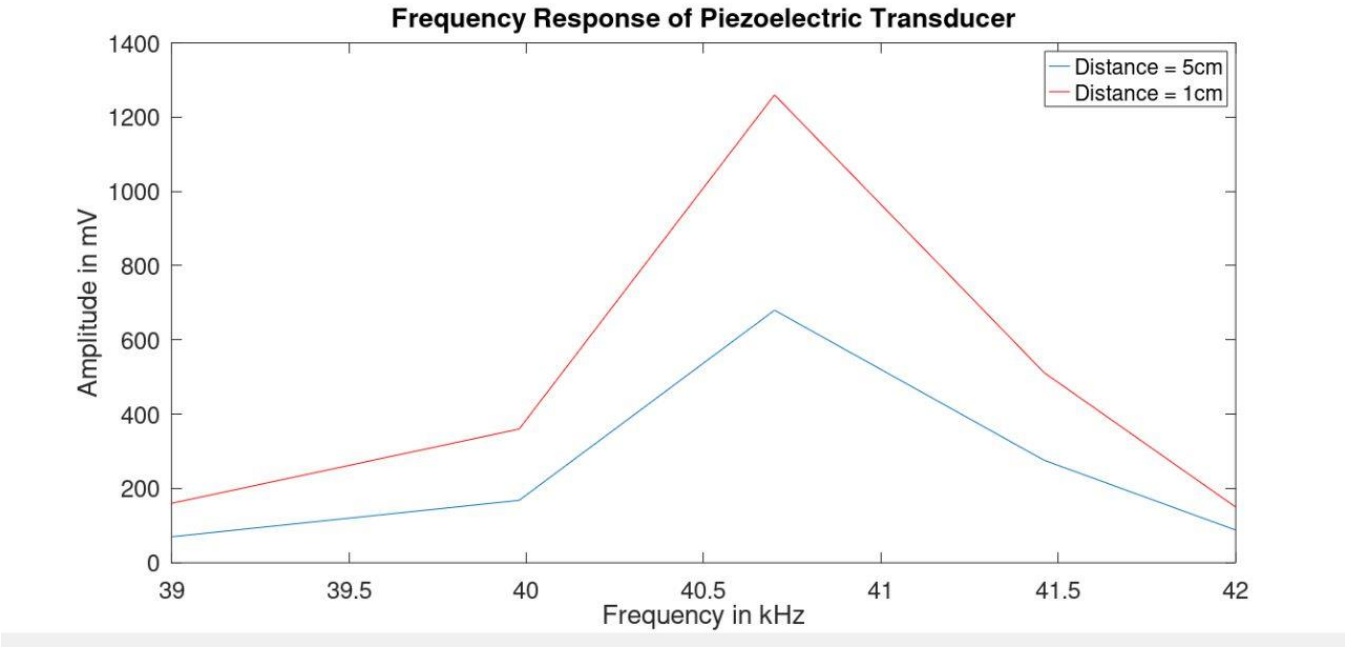

Figure 5.2: - Frequency Response Graph of the Piezoelectric Transducer, where the Amplitude of the Received signal is Maximum at 40.7 KHz

5.3 Bandpass Filter characteristics of UAM

The Bandpass Filter characteristics in Fig 5.3 depicts that the Frequency range it passes is 38-43 KHz.

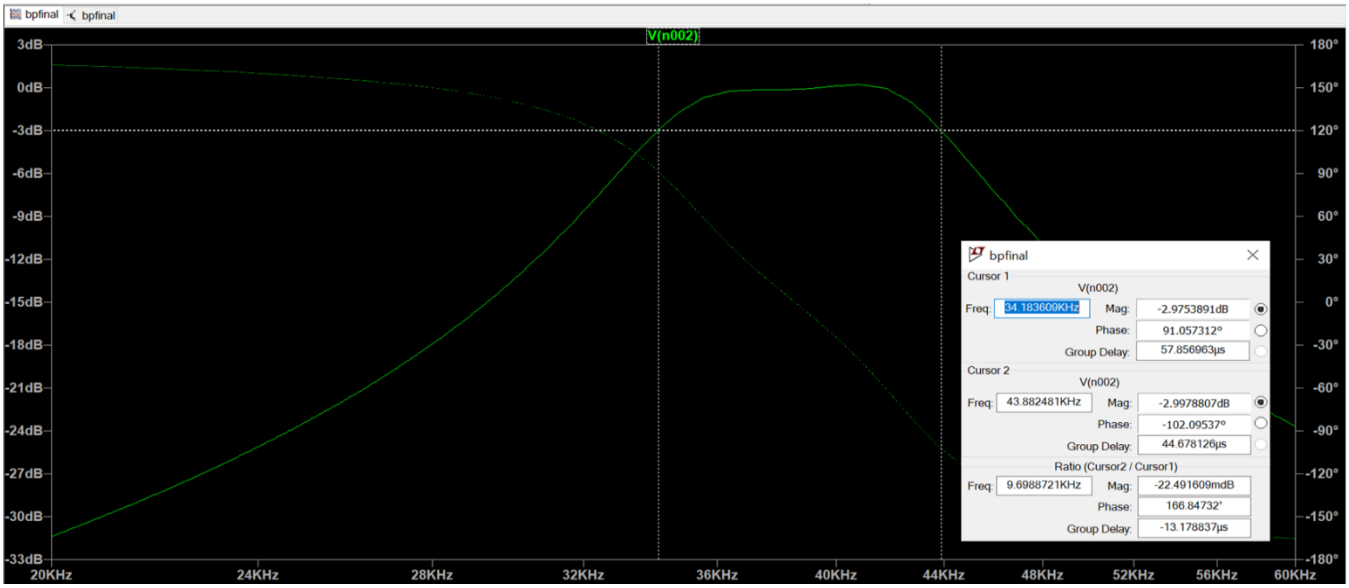

Figure 5.3: - Frequency Response Graph of Bandpass Filter

5.4 Output of Dual Rail Power Supply

The output characteristics load resistance is varied and the corresponding value of virtual ground is noted. It is inferred that for larger value of resistance, virtual ground differs from actual ground by 2mV (offset voltage of LM324 IC).

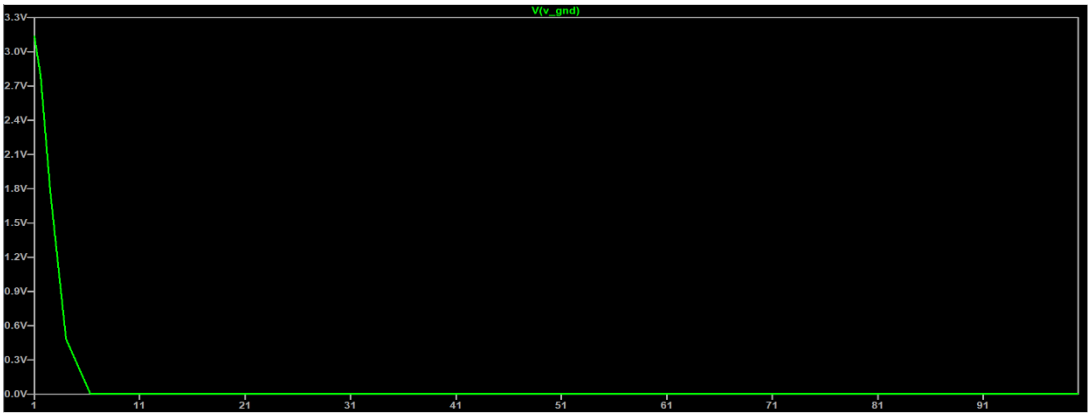

Figure 5.4: - Load vs Voltage Graph of Dual Rail Power Supply

5.5 Footprint design of UAM PCB

The UAM PCB is designed using Kicad and the footprint is shown in Fig 5.5. 10x 1 male connecter is used for easier connection with microcontroller and dual rail power supply.

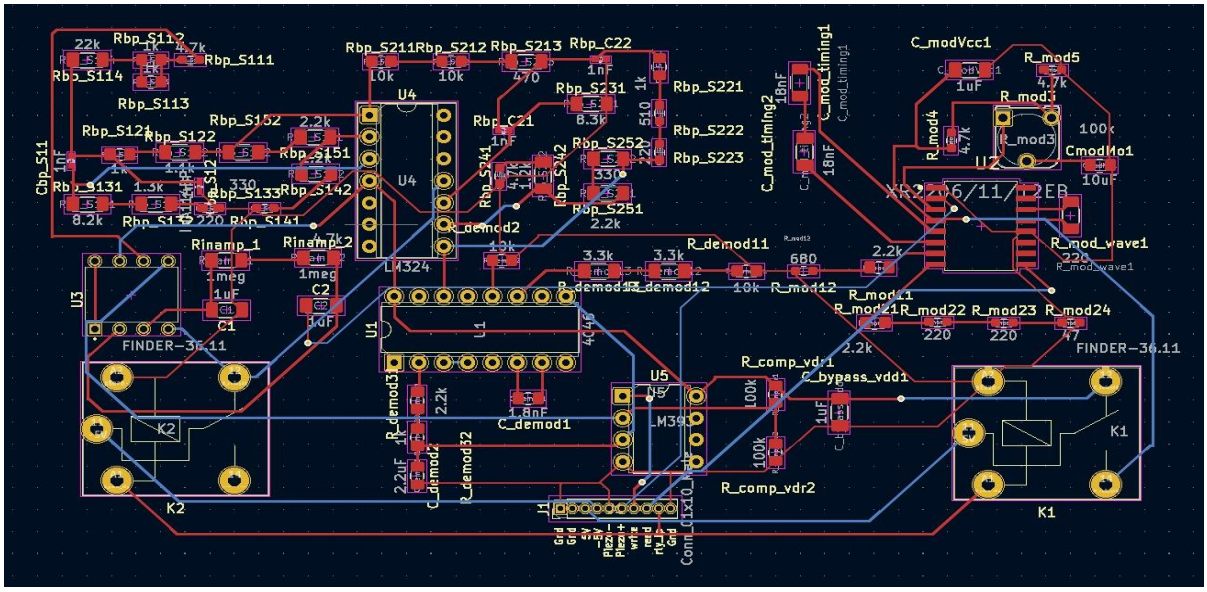

Figure 5.5: - Footprint of the UAM PCB

5.6 Contents of the schematic of the UAM

The 3D View of the UAM using Kicad is shown in Fig 5.6.

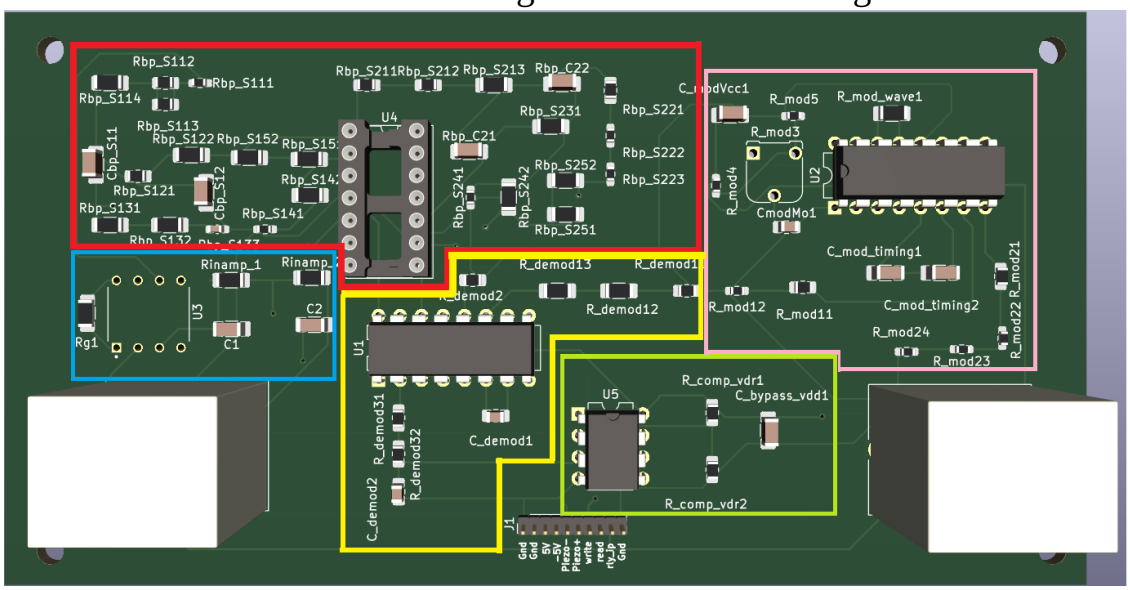

Figure 5.6: - Kicad schematic contents of the UAM

5.7 Board Statistics of UAM PCB

From figure 5.7 gives Board Statistics of FSK modem which has 8632.5 mm^2 board area. 9 through holes components (THT) and 57 Surface Mount Devices (SMD) gives total of 67 components with majority of components is SMD Resistors and Capacitors.

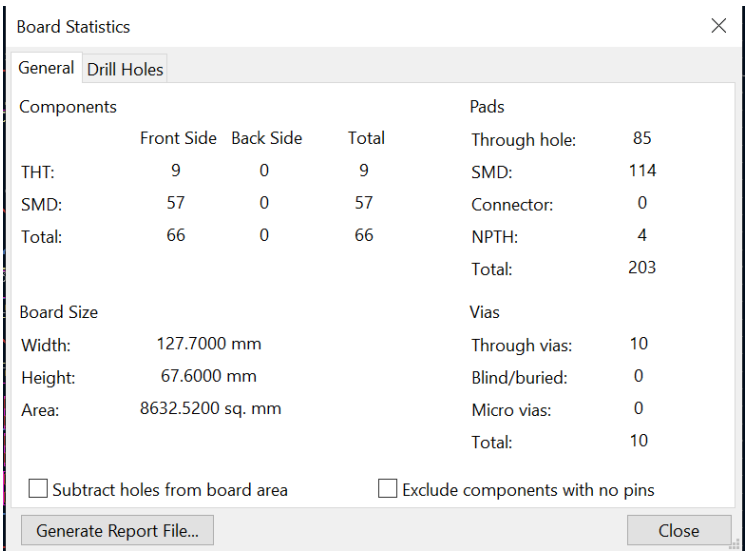

Figure 5.7: - Board Statistics for UAM PCB

5.8 Footprint design of UAM Power Supply PCB of UAM

The Kicad Footprint of UAM Power Supply Board and the footprint is shown in Fig 5.8.

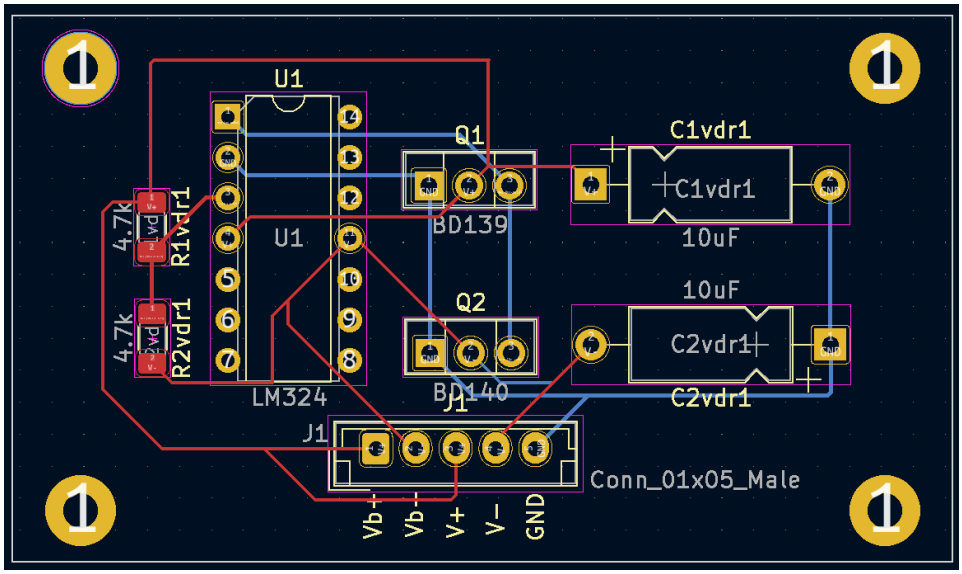

Figure 5.8: - Footprint of Power Supply PCB of UAM

5.9 Contents of the schematic of the Power Supply PCB of UAM

The 3D View of the Power Supply Board of UAM using Kicad is shown in Fig 5.9.

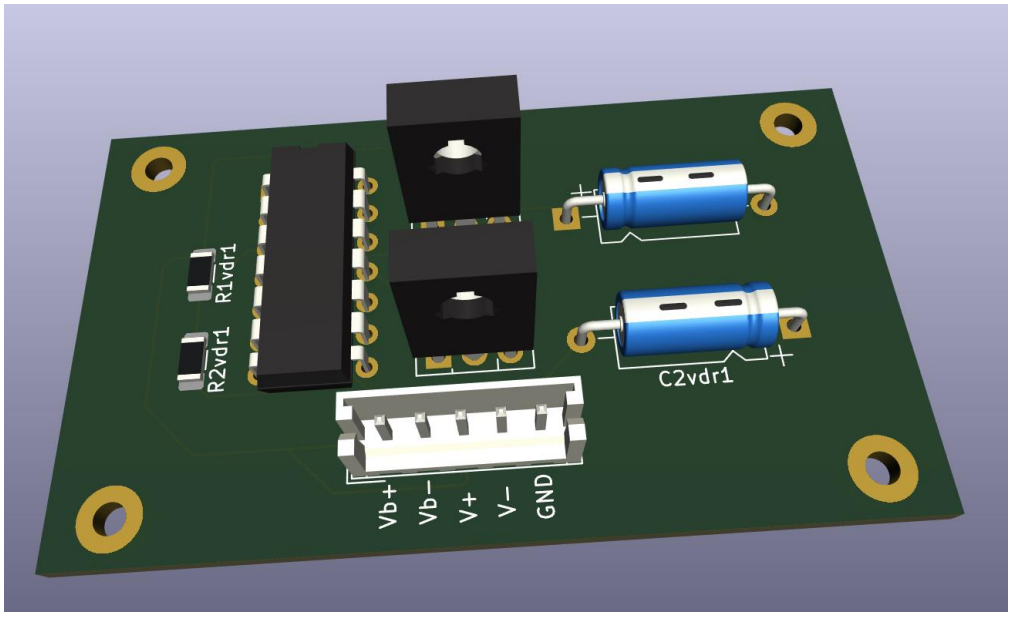

Figure 5.9: - KiCad schematics contents of Power Supply PCB of UAM

5.10 Board Statistics of Power Supply PCB of UAM

Figure 5.10 shows Dual Rail Power Supply Board Statistics which has 2016 mm^2 board area. 6 through holes components (THT) and 2 Surface Mount Devices (SMD).

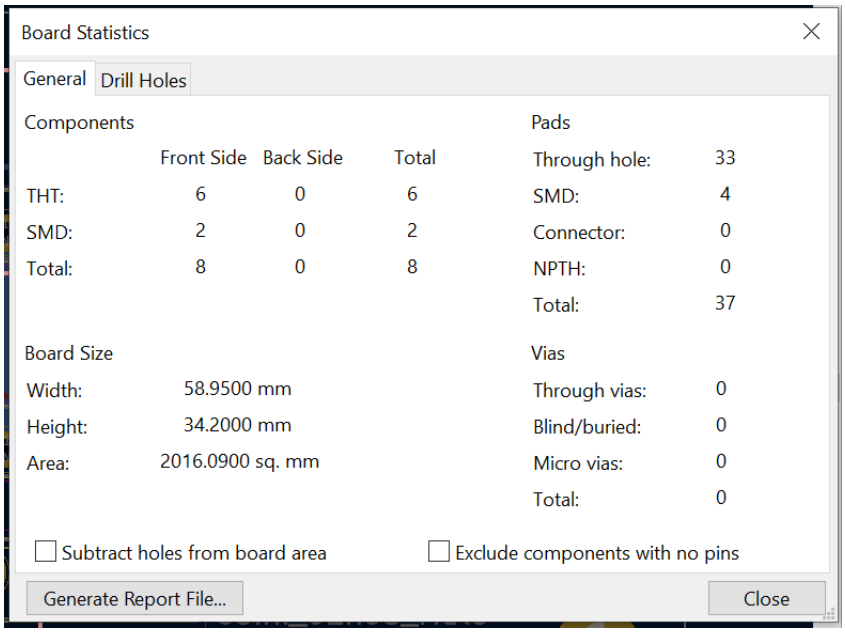

Figure 5.10: - Board Statistics for Power Supply PCB of UAM

5.11 Cost Estimation for UAM

The aim of this project was to design a low cost underwater acoustic modem. The UAM was built components currently available in the market. The cost estimation table is given Table 6.1.

Table 5.1: - Cost Estimation of UAM

Component Name	Cost
Preamplifier	315
Bandpass filter	80
FSK Modulator	150
Dual Power Rail	60
Li-ion cells	750
FSK Demodulator	65
Piezo electric transducer	500
Buck boost converter	120
STM32F103C8T6	300
BMS	105
Total	2445

The cost analysis of the UAM is given in Table 5.1. As per the cost analysis pie chart of FSK Modem (fig 5.12), Li ion cells costs nearly 1/3 of total modem cost followed by Piezo electric transducer (1/5th total cost) and Pre-Amplifier and so on. From the fig Total cost comes 2500 Rupees.

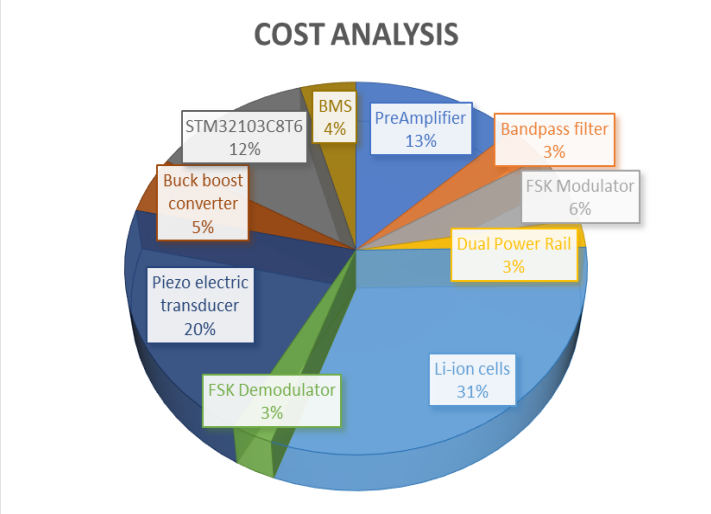

Figure 5.12: - Cost Analysis of UAM

CHAPTER 7
CONCLUSION

The proposed describes the design and technical parameters of a low-cost Underwater Acoustic Modem, which is based on open-source resources for the technology to be available to everyone and so that future generations may work on upgrading it. The modem is designed to be worked in shallow water (around 100m) depth and prioritizes reliability over performance.

The project is in the hardware and software simulation phase. The KiCad and LTSpice simulations have verified the working of the components. The next step is to progress this design to a working modem that can emit and receive acoustic signals, thereby forming an underwater Acoustic Communication Network between other Underwater Acoustic Modems.

REFERENCES

[1] Emrecan Demirors, George Sklivanitis, G. Enrico Santagati, Tommaso Melodia, Stella N. Batalama, “Design of A Software-defined Underwater Acoustic Modem with Real-time Physical Layer Adaptation Capabilities”, WUWNET '14: Proceedings of the International Conference on Underwater Networks & Systems November 2014 Pages 1–8.

[2] J. G. Duarte-Junior_, F. A. Brito-Filhoy (2021), “A Multimode FPGA-based Modem with Embedded Analog-to-Digital Converter for Software Defined Radio”, 2021 Wireless Telecommunications Symposium (WTS), ISBN:978-1-7281-8480-7.

[3] B. Benson, Y. Li, R. Kastner, B.Faunce, K. Domond, D. Kimball, C. Schurgers, (2010) “Design of a Low-Cost, Underwater Acoustic Modem for Short review-Range Sensor Networks” , ISBN : 978-1-4244-5222-4.

[4] Henrique Manuel, Pereira Cabral (2014), “Acoustic modem for underwater communication”.

[5] Jurdak, R., Lopes, C. V., & Baldi, P. (2006). “Software Acoustic Modems for Short Range Mote-based Underwater Sensor Networks”, OCEANS 2006 - Asia Pacific. DOI:10.1109/oceansap.2006.4393864, ISBN:978-1-4244-0137-6.

[6] Siyuan Zheng, Feng Tong, Bin Li, Qiuyang Tao, Aijun Song and Fumin Zhang, “Design and Evaluation of an Acoustic Modem for a Small Autonomous Unmanned Vehicle”, Sensors (Basel). 2019 Jul; 19(13): 2923.

[7] Slamet Indriyanto, Anggun Fitrian Isnawati, Jans Hendry, Ian Yosef Matheus Edward (2020), “Underwater Data Transmission Using Frequency Shift Keying (FSK) Modulation with Bit Rate of 2400 bps”, Buletin Pos dan Telekomunikasi Vol. 18 No.1 (2020): 17-28, DOI: 10.17933/bpostel.2020.180102.

[8] STMicroelectronics. (2008, July). STM32F1 Discovery Datasheet.

[9] JSN-SR04T Datasheet. (2018, May).

[10] Benjamin Sherlock, Nils Morozs, Jeffrey Neasham and Paul Mitchell (2022), “Ultra-Low-Cost and Ultra-Low-Power, Miniature Acoustic Modems Using Multipath Tolerant Spread Spectrum Techniques”, p.1-25, Electronics 2022, 11, 1446.

[11] Heungwoo Nam, Sunshin An (2007), “An Ultrasonic Sensor Based Low-Power Acoustic Modem for Underwater Communication in Underwater Wireless Sensor Networks”, Emerging Directions in Embedded and Ubiquitous Computing. EUC 2007, LNCS 4809, pp. 494–504, 2007.

[12] Antonio Sánchez, Sara Blanc, Pedro Yuste, Angel Perles and Juan José Serrano “An Ultra-Low Power and Flexible Acoustic Modem Design to Develop Energy-Efficient Underwater Sensor Networks”, Sensors 2012, 12, 6837-6856; doi:10.3390/s120606837

[13] Tae-Hee Won 1, Sung-Joon Park, "Design and implementation of an omni-directional underwater acoustic micro-modem based on a low-power micro-controller unit", Sensors (Basel). 2012;12(2):2309-23. doi: 10.3390/s120202309. Epub 2012 Feb 20.

[14] Kaizhuo Lei, Xuchao Fan, Xintong Ren, Qunfei Zhang (2017), “Research on high performance low power AGC circuit based on AD8338”, 2017 IEEE International Conference on Signal Processing, Communications and Computing (ICSPCC), ISBN:978-1-5386-3142-3, DOI: 10.1109/ICSPCC.2017.8242616.

[15] Sumithra G, Meganathan D, “A study on unpredictable shallow water channel behavior by various multipath patterns and experimental data analysis”, Journal of Engg. Research Vol.9 No. (4B) December 2021 pp. 70-82, DOI:10.36909/jer.9669.

[16] Abolfazl Falahati, Bryan Woodward, and Stephen C. Bateman,“Underwater

Acoustic Channel Models For 4800 b/s QPSK Signals", IEEE Journal of Oceanic Engineering (Volume: 16, Issue: 1, January 1991), ISSN: 0364-9059, DOI: 10.1109/48.64881.

[17] Jennifer Trezzo (2013), "Design and Implementation of an Adaptive Underwater Acoustic Modem and Test Platform", University of California, San Diego.

[18] Suresh Kumara and Chanderkant Vatsb," Underwater Communication: A Detailed Review", 2889.

[19] Eric Gallimore, Jim Partan, Ian Vaughn, Sandipa Singh, Jon Shusta, Lee Freitag, "The WHOI Micromodem-2 (2010): A Scalable System for Acoustic Communications and Networking", OCEANS 2010 MTS/IEEE SEATTLE, doi:10.1109/OCEANS. 2010.5664354.

[20] Qian Lu, Jiang Shengming (2016), "A Review of Routing Protocols of Underwater Acoustic Sensor Networks from Application Perspective", 2016 IEEE International Conference on Communication Systems (ICCS), ISBN: 978-1-5090-3423-9, DOI: 10.1109/ ICCS.2016.7833633.

[21] Linear Technology. LT8362 Low IQ Boost/SEPIC/Inverting Converter with 2A, 60V Switch, Data Sheet (Rev. B), 2017.

[22] Analog Devices, LTC4444: High Voltage Synchronous N-Channel MOSFET Driver Data Sheet (Rev. C), 2011.

[23] STB70N10F4, STD70N10F4STP70N10F4, STW70N10F4 N-channel 100 V, 0.015 Ω, 60 A, STripFET™ DeepGATE™ Power MOSFET in TO-220, DPAK, TO-247, D2PAK Datasheet.

[24] Analog Devices, AD5241/AD5242: I2C-Compatible, 256-Position Digital Potentiometers Data Sheet (Rev. E), 2000.

[25] Analog Devices, AD8338: Low Power, 18 MHz Variable Gain Amplifier Data Sheet (Rev. C), 2013.

[26] Analog Devices, ADA4805-1/ADA4805-2: 0.2 μV/°C Offset Drift, 105 MHz Low

Power, Low Noise, Rail-to-Rail Amplifiers Data Sheet (Rev. B), 2014.
[27] Analog Devices, AD5246: 128-Position I2C-Compatible Digital Resistor Datasheet (Rev. C), 2006.
[28] Mandar Chitre, "Unetstack, Underwater Networks Handbook Version 3.3.0", 2021.
[29] Analog Devices. In-Amp Diamond Plot Tool.
[30] Chethan B, Ravisimha B N, Dr. M Z Kurian (2014), “The effects of Inter Symbol Interference (ISI) and FIR Pulse Shaping Filters: A survey”, International Journal of Advanced Research in Electrical, Electronics and Instrumentation Engineering, Vol. 3, Issue 5.
[31] Himanshu Jindal, Sharad Saxena, Singara Singh (2014), “Challenges and Issues in Underwater Acoustics Sensor Networks: a review”, 2014 International Conference on Parallel, Distributed and Grid Computing, ISBN: 978-1-4799-7683-6.
[32] Application Note AN-1071 Class D Audio Amplifier Basics by Jun Honda & Jonathan Adams – International IOR Rectifier, 2005
[33] Gregory Sharp (2014), “Sepic Converter Design and Operation”.
[34] Chi-fang Chen, Kai-Jen Hsiao, Sheng-yu Chuang, Chia-Lu Hu (2015), “Establishment of a robust Underwater Acoustic Repeater with applications in Underwater Acoustic Transmission and Detection”, OCEANS 2015 – Genova, ISBN: 978-1-4799-8736-8, DOI: 10.1109/OCEANS-Genova.2015.7271770.
[35] Oluwaseyi Onasami, Damilola Adesina, Lijun Qian (2021), “Underwater Acoustic Communication Channel Modeling using Deep Learning”, WUWNet'21: The 15th International Conference on Underwater Networks & Systems, (9): 1–8.
[36] Analog Devices -Analog Filter Wizard - ADI Precision Studio
[37] F. De Rango, F. Veltri, P. Fazio (2012), “A Multipath Fading Channel Model for Underwater Shallow Acoustic Communications”, IEEE ICC 2012 - Signal Processing for Communications Symposium, ISBN: 978-1-4577-2053-6.
[38] Paul Ozog, Miriam Leeser, Milica Stojanovic (2009), “Adapting the USRP as an

Underwater Acoustic Modem".

[39] Simon Haykins & Michael Moher, "Modern Wireless Communications", Pearson Education, 2007.

[40] Muhammad H.Rashid, "Power Electronics", Pearson Education / PHI , 2004.

[41] Oluwaseyi Onasami 1, Ming Feng2, Hao Xu 3, Mulugeta Haile4,
And Lijun Qian 1 (2022), "Underwater Acoustic Communication Channel Modeling Using Reservoir Computing", IEEE Access, Volume 10.

[42] Adel.S. Sedra, Kenneth C. Smith, "Micro Electronic Circuits", 7th Edition, Oxford University Press, 2014.

[43] M. S. Martins, N. Pinto, J. P. Carmo and J. Cabral (2014), "High Data Rate Acoustic Modem for Underwater Aplications", ISBN: 978-1-4799-3743-1.

[44] Nam-Yeol Yun, Yung-Pyo Kim, Sardorbek Muminov, Jin-Young Lee, Soo-Young Shin, and Soo-Hyun Park (2011), "Sync MAC Protocol to control Underwater Vehicle based on Underwater Acoustic Communication", ISBN: 978-0-7695-4552-3.

[45] Linear Technology (2011) LT1167 Single Resistor Gain Programmable, Precision Instrumentation Amplifier Datasheet.

[46] Analog Devices. OP282/OP482 Dual/Quad, Low Power, High Speed JFET Operational Amplifiers Datasheet (Rev. I), 2010.

[47] B.Pranithaa, L.Anjaneyulu (2020) "Analysis of Underwater Acoustic Communication System Using Equalization Technique for ISI Reduction", International Conference on Computational Intelligence and Data Science (ICCIDS 2019), Procedia Computer Science 167 1128–1138.

[48] SamacSys, "Electronic Component CAD models – Symbols | Footprints | 3D Models", www.samacsys.com. G. V. V. Pavan Kumar, V. V. S. Prasad & U. S. Ramesh (2021), "Underwater noise levels in Indian waters off the coast of Mormugao Port", Journal of operational oceanography, VOL. 14, NO. 1, 48–58.

[49] STMicroelectronics. (2012, May). STM32F4 Discovery Datasheet.

[50] Exar Corporation. (2013, July). XR2206 Monolithic Function Generator Datasheet.

[51] Texas Instruments. (2019, November). CD4046B Phase-Locked Loop: A Versatile Building Block for Micropower Digital and Analog Applications Datasheet.